cosmetics

MDPI

Article

Non-Invasive Assessment of Skin Barrier Properties: Investigating Emerging Tools for In Vitro and In Vivo Applications

Emer Duffy [1], Keana De Guzman [1], Robert Wallace [2], Ronan Murphy [2] and Aoife Morrin [1,*]

[1] School of Chemical Sciences, National Centre for Sensor Research, Insight Centre for Data Analytics, Dublin City University, D09 W6Y4 Dublin 9, Ireland; emer.duffy@dcu.ie (E.D.); keana.deguzman2@mail.dcu.ie (K.D.G.)

[2] School of Health and Human Performance, Dublin City University, D09 W6Y4 Dublin 9, Ireland; robertwallace7@hotmail.com (R.W.); ronan.murphy@dcu.ie (R.M.)

* Correspondence: aoife.morrin@dcu.ie; Tel.: +353-1-700-6730

Received: 20 August 2017; Accepted: 20 October 2017; Published: 24 October 2017

Abstract: There is increasing interest in the development of non-invasive tools for studying the properties of skin, due to the potential for non-destructive sampling, reduced ethical concerns and the potential comparability of results in vivo and in vitro. The present research focuses on the use of a range of non-invasive approaches for studying skin and skin barrier properties in human skin and human skin equivalents (HSE). Analytical methods used include pH measurements, electrical sensing of the epidermis and detection of volatile metabolic skin products. Standard probe based measurements of pH and the tissue dielectric constant (TDC) are used. Two other more novel approaches that utilise wearable platforms are also demonstrated here that can assess the electrical properties of skin and to profile skin volatile species. The potential utility of these wearable tools that permit repeatability of testing and comparability of results is considered through application of our recently reported impedance-based tattoo sensors and volatile samplers on both human participants and HSEs. The HSE exhibited a higher pH (6.5) and TDC (56) than human skin (pH 4.9–5.6, TDC 29–36), and the tattoo sensor revealed a lower impedance signal for HSEs, suggesting the model could maintain homeostasis, but in a different manner to human skin, which demonstrated a more highly resistive barrier. Characterisation of volatiles showed a variety of compound classes emanating from skin, with 16 and 27 compounds identified in HSEs and participants respectively. The continuing development of these tools offers potential for improved quality and relevance of data, and potential for detection of changes that are undetectable in traditional palpable and visual assessments, permitting early detection of irritant reactions.

Keywords: living skin equivalent; skin barrier function; wearable; epidermal tattoo sensor; hydration; pH; volatile organic compounds; gas chromatography-mass spectrometry; impedance spectroscopy

1. Introduction

The development of new methods and instrumental techniques is crucial for the growing cosmetics sector. Non-invasive technologies can enable comparability of results (i.e., between model vs. human studies) compared to invasive techniques that are typically destructive, and which inhibit the ability of investigators to repeat their measurements or perform frequent comparisons. Cosmetic product testing is also most informative when carried out in human participants, thus supporting the advancement of non-invasive analytical tools. There is a growing interest in the development of such technologies for interrogating the properties of human skin for a variety of

applications, including skin physiology research [1,2], diagnostics and therapy [3], personal wearable devices [4], and cosmetic testing [5–7].

Skin physiology and the skin barrier are especially significant in cosmetic dermatology. All cosmetic products impact the barrier, either beneficially through the improvement of skin hydration and barrier repair, or negatively through irritant-induced contact dermatitis. Commonly used methods for assessment of skin barrier function (SBF) include determination of stratum corneum (SC) water content, trans-epidermal water loss (TEWL) and skin pH. Optical coherence tomography and Raman spectroscopy have also emerged in recent years as complementary methods to assess SBF [8]. The present research focuses on two emerging non-invasive approaches for investigating skin physiology and SBF; epidermal sensing platforms and volatile metabolic products. Their potential utility as tools that permit repeatability of testing as well as comparability of results (i.e., towards applications both in vitro and in vivo) is considered herein.

Temporary tattoo sensors offer a promising non-invasive approach to monitoring the physical and chemical properties of skin. They are a type of wearable epidermal sensing platform that employs electrically conducting materials that conform intimately to the mechanics of skin and deliver good electrical performance [9]. They are inexpensive, simple to fabricate and can be used to measure a wide variety of parameters. For example, Jia et al. have demonstrated lactate sensing in sweat using a temporary tattoo amperometric sensing approach [10], and Bandodkar et al. have demonstrated an enzyme based tattoo amperometric epidermal sensor for glycemic level monitoring during food consumption [11]. Our group has recently reported a screen-printed temporary tattoo sensor for non-invasive skin barrier assessment using impedance spectroscopy [12]. Impedance spectroscopy allows for non-invasive measurements of the overall resistance and reactance of skin using alternating current of various frequencies, where electrical impedance of intact skin is dominated by the SC at low frequencies ($\leq$1 KHz) [13]. The electrical properties of the SC of living skin equivalents and human skin were impedimetrically assessed herein using screen-printed tattoo electrodes.

Another emerging non-invasive approach offering unique insights into ongoing physiological processes in skin is the monitoring of volatile organic compounds (VOCs). The human body emits hundreds of volatile metabolic products (via breath, blood, urine, faeces and skin), which contain the footprints of cellular activities and can thus reveal those pathologies that alter the metabolism [14]. A compendium of 1840 volatiles contributing to the volatilome in healthy humans was recently published [15]. Skin VOCs are of great interest in many fields, from cosmetics (e.g., design of fragranced products) [16] to diagnostics [17], forensics and criminal investigations [18], and the ecology of blood-sucking insect vectors of human disease [19]. Recent reports have highlighted the significance of VOCs for skin physiology and pathophysiology research, where differential expressions of volatiles were demonstrated in melanoma vs. naevi and normal skin [20], and in compressed vs. uncompressed tissue towards early detection of pressure ulcer formation [21]. Our group has recently demonstrated the potential of VOCs for skin physiology and SBF research where discriminating volatile emissions were observed before and after acute barrier disruption [22]. Collection and analysis of VOCs from skin is commonly achieved using solid-phase microextraction (SPME) [23] in combination with gas chromatography-mass spectrometry (GC-MS) [24] owing to the sensitivity of mass spectrometry, and the ease of performing headspace (HS) sampling with SPME.

The first application these emerging tools to the characterisation of 3D HSEs is reported herein, towards developing an understanding of the biophysical and biochemical properties that can be accessed non-invasively and to establish a baseline dataset for future studies. Headspace SPME with GC-MS was utilised for volatile analysis, and temporary tattoo sensors for investigation of SC electrical properties. A concurrent investigation of human skin was conducted to investigate these two tools for in vitro and in vivo assessments, regarding their potential to permit repeatable analysis and evaluation of the comparability between in vitro and in vivo models.

2. Materials and Methods

2.1. Living Skin Equivalents

Labskin full thickness living skin equivalent (Batch 170105) was obtained from Innoven UK Ltd. (www.innovenn.co.uk/labskin, York, England, UK). Labskin has a robust structure owing to the use of fibrin in constructing a synthetic dermal matrix, which contains primary human fibroblasts. It has a well-differentiated, air-exposed epidermis composed of neonatal foreskin primary human keratinocytes. The living skin equivalents measured 24 mm in diameter. All living skin equivalents were incubated at 37 °C in 5% (*v*/*v*) carbon dioxide and air. Labskin remains viable for ~10 days after reception, thus providing a 10-day test window which informed the sampling strategy herein.

2.2. Human Participants

Healthy volunteers were recruited (4 females age 22–28, 4 males age 22–25; non-smokers except for M2) for the tissue dielectric, pH and volatile measurements. No special dietary regimes were applied, however, participants were instructed not to apply perfumes of cosmetics on their hands or arms on the days of sample collection. The local ethics committee (Dublin City University Research Ethics Committee, DCUREC/2016/053) approved the study on skin volatiles prior to commencement of the work, and the study was performed according to the Declaration of Helsinki. Participants were informed on the aims of the study and asked to provide written informed consent before their involvement. Before samples were collected from skin, participants washed their hands and arms with tap water, followed by drying with paper towels to minimise contributions from trace cosmetics or other exogenous compounds on the skin. For the tattoo-based impedance measurements, informed consent was received from all participants (4 females, 4 males; age 22–28).

2.3. Tissue Dielectric and pH Measurements

Tissue dielectric constants (TDC) were measured on human skin (volar forearm) and Labskin within a laminar flow cabinet using a Delfin MoistureMeter D, a commercial skin hydration probe (Delfin Technologies, Kuopio, Finland). Each measurement was repeated 3 times using the extra small probe (effective measuring depth of 0.5 mm). The Delfin probe was cleaned with 70% ethanol solution between measurements. A Hanna 2210 pH meter with a HI1413 probe (Hanna Instruments Inc., Bedfordshire, UK) was used to investigate the pH of human skin (volar forearm) and Labskin, and each measurement was repeated three times. The pH probe was cleaned with 1 M sodium hydroxide between measurements. TDC and pH were characterised for Labskin and human skin over a 10-day period, where measurements were made on days 1, 3, 6, 7, 8 and 10.

2.4. Temporary Tattoo Sensors and Impedance Measurements

A 2-concentric circle design was employed for tattoo sensors, which were screen-printed (DEK semi-automated 248 screen-printer) from silver paste ink (PF-410 ink, Nor-Cote International Ltd., Eastleigh Hampshire, England) on temporary transfer tattoo paper substrates (Sports Ink^{TM}, Dublin, Ireland). The tattoo dimensions were 20 mm diameter with inner and outer electrodes separated by a distance of 3 mm. After printing, the electrodes were cured at 120 °C for 5 min. The tattoos were applied on Labskin and human skin (male and female participants) (volar forearm) by placing the design face down and dabbing the backing paper with water for 1 min. The backing paper releases an ethylcellulose layer (EC) resulting in the electrodes adhering to the skin's surface, covered by the EC layer. Skin hydration was analysed using the impedance spectroscopy approach [25], with an Autolab PGSTAT128N workstation. Two gold pins were soldered 7 mm apart on to a strip board (Maplin Electronics, Dublin, Ireland) and used to contact the inner and outer tattoo electrodes to connect to the potentiostat. The frequency range scanned was from 0.1 Hz to 1 MHz with amplitude 0.03 V. All spectra collected were recorded at 0.1 V set potential.

2.5. Headspace Sampling and Gas Chromatography-Mass Spectrometry Analysis of Volatiles

Solid-phase microextraction (SPME) fibres were used for sampling volatiles in the skin headspace. They comprised of 50/30 µm divinylbenzene/carboxen/polydimethylsiloxane Stableflex (2 cm) assemblies (Supelco Corp., Bellefonte, PA, USA). The SPME fibre was housed within a glass holder that was affixed to the volar forearm with Leukosilk surgical tape (BSN Medical GmbH, Hamburg, Germany). This comprised of a glass funnel (3 mL volume, Pyrex®, Fisher Scientific Ireland, Blanchardstown, Dublin, Ireland) and two septa (Supelco Thermogreen LB-2 Septa plug, Sigma Aldrich, Arklow, Ireland). This served to hold the SPME fibre in an enclosed area of skin headspace, where sample collection took place for 15 min. For volatile sampling Labskin, the SPME fibre was housed in a similar manner within a funnel with two septa, and placed over the Labskin well plate within the incubator, where sample collection took place for 15 min. Labskin and human skin VOCs were studied over a 10-day period, where HS samples were collected on days 1, 3, 6, 7, 8 and 10. Samples were subsequently analysed using gas chromatography-mass spectrometry (GC-MS), where an Agilent 6890 gas chromatograph connected to an Agilent 5973 mass selective detector was used. The system was equipped with a SPME Merlin Microseal (Merlin Instrument Company, Newark, DE, USA) and separations were performed on an SLB-5ms column (30 m $\times$ 0.25 mm $\times$ 0.25 µm d_f, Supelco, Bellefonte, PA, USA). Helium carrier gas was used at a constant flow rate (1 mL/min). The inlet was maintained at 250 °C (splitless mode), and SPME fibres were desorbed for 2 min within a SPME inlet liner. The GC oven temperature was 40 °C for 5 min, after which the oven was programmed at a rate of 15 °C/min to 270 °C. The MS was operated at a scan rate of 3.94 s^{-1}, with a scan range of 35–400 m/z, ion source temperature 230 °C and ionising energy of 70 eV. Data were analysed using Agilent GC/MSD ChemStation and OpenChrom® (Lablicate GmbH, Hamburg, Germany) [26]. The identification of compounds was performed using the National Institute of Standards and Technology Library, and was supported by retention index matching. A standard mixture of saturated alkanes (C_7–C_{30}, Sigma Aldrich, Arklow, Ireland) was used for retention index matching.

3. Results and Discussion

3.1. Biophysical Properties and Temporary Tattoo Sensors

HSEs mimic key elements of human skin biology and overcome the limitations associated with monolayer tissue culture, such as a failure to capture the complexity of the in vivo microenvironment and cell-cell interactions [27]. They permit a more detailed study of skin physiology while providing an important intermediate step in direct studies on skin, as well as an ethical, time- and cost-effective alternative to the use of laboratory animals. Labskin is a HSE that consists of a fully differentiated epidermis on a dermal compartment composed of polymerised fibrin containing primary human keratinocytes (Figure 1a). The larger diameter (24 mm) and robust structure (Figure 1b) permitted facile interrogation of the properties of this HSE, wherein screen-printed tattoo sensors could be applied directly on the model surface (Figure 1c), and collection of VOCs in the headspace could be accomplished by simply placing the SPME sampling funnel directly over the model. Collection of VOCs could easily be performed on differently sized HSEs by adjusting the size of the headspace, however, the current tattoo format is 20 mm diameter and would require modification for use in smaller HSEs. The biophysical properties of Labskin were also characterised; local tissue hydration levels were investigated as a function of tissue dielectric constants (TDC) and surface pH was measured. A parallel analysis was conducted on human skin towards understanding repeatability of testing as well as comparability of results.

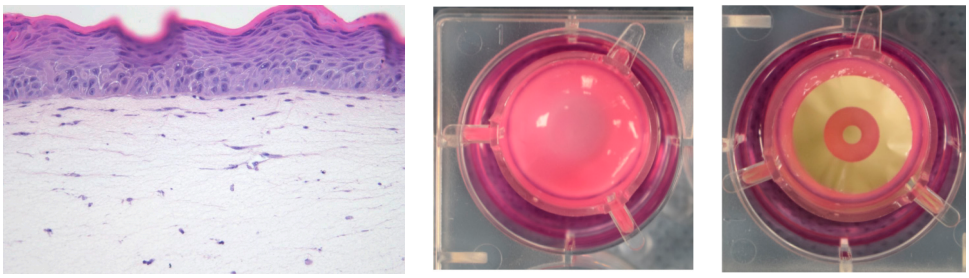

(**a**) (**b**) (**c**)

Figure 1. (**a**) Hematoxylin and eosin stained paraffin embedded living skin equivalent (Image courtesy of Innoven UK Ltd.); (**b**) The 24 mm diameter living skin equivalent model in use; (**c**) Tattoo sensor applied to the surface of Labskin.

Labskin exhibited an acidic surface, with an average pH of 6.5 ± 0.2. This was higher than that measured for human skin, which measured an average pH of 4.9 ± 0.4 and 5.6 ± 0.3 for male and female participants respectively (Figure 2a). The reported range for normal human skin varies from an acidic pH of 3.0 to a near neutral pH of 6.5, and is affected by numerous factors [28]. Similar HSE models have demonstrated the same range of acidic surface pH (pH 6.3), which was higher than that measured for human skin (pH 5.4) [29].

Labskin also displayed barrier integrity with a TDC of 56.3 ± 5.7. This was higher than that measured for human skin; 36.0 ± 4.0 for male and 29.4 ± 2.1 for female participants (Figure 2b). This is in agreement with previous reports on a similar HSE where higher TEWL (60 $g \cdot m^2 \cdot h^{-1}$ in vitro vs. 10–45 $g \cdot m^2 \cdot h^{-1}$ in vivo) values were recorded [29]. Measured human TDC values were also within the normal range, where men typically exhibit higher TDC than women [30]. The higher degree of variability observed for TDC in Labskin could be accounted for by the fact that the HSE was removed from the controlled humidity environment to perform measurements. Establishing an understanding of these biophysical properties and their normal range is important as it provides a baseline for future research, and has relevance for studies into areas ranging from product testing to skin physiology, the microbiome and barrier function where environmental conditions, pH, TDC and gender can play a pivotal role [31].

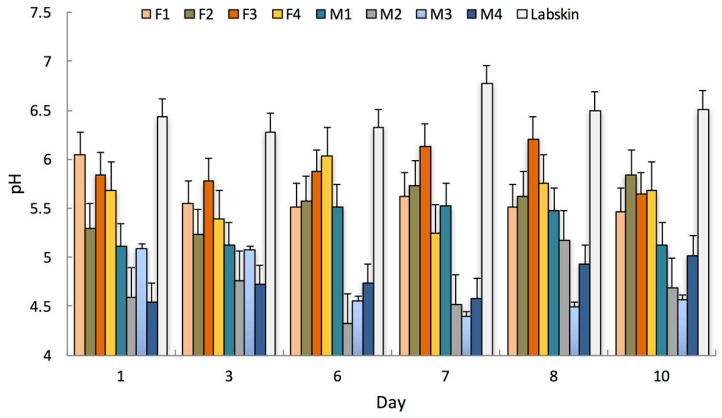

(**a**)

Figure 2. *Cont.*

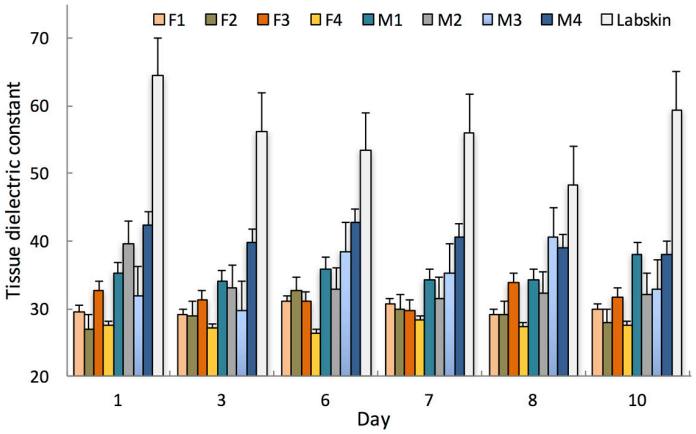

(**b**)

Figure 2. (**a**) Measured pH values for Labskin and human participants' skin over a 10-day period; (**b**) Measured tissue dielectric constants (TDC) for Labskin and human participants' skin over a 10-day period. (F = female, M = male, Error bars represent the 95% confidence interval, n = 3).

The barrier electrical properties of Labskin and human skin were impedimetrically assessed using screen-printed tattoo electrodes and the impedance data is presented as Bode and Nyquist plots (Figure 3). A Nyquist plot visualises the data as a complex plane by plotting the real (Z′) and imaginary (Z″) with every point providing a characteristic feature at a certain frequency. In comparison, the Bode plot showcases the amplitude/magnitude and the phase over the frequency range analysed, which is an advantageous compared to the Nyquist plot where frequency is not explicitly presented.

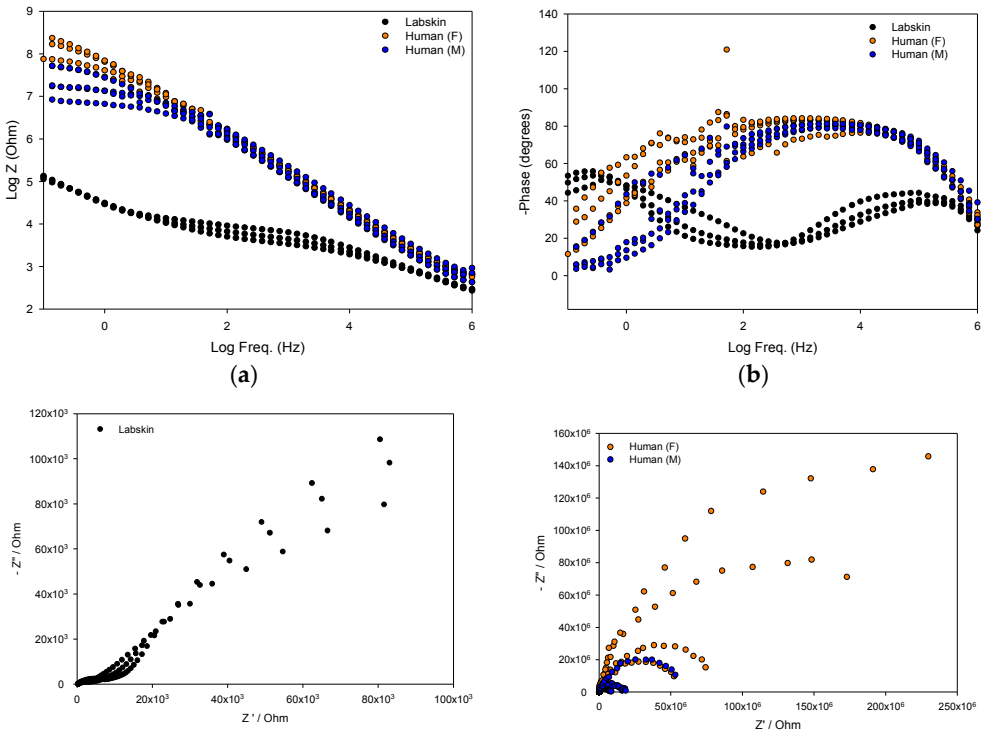

Figure 3. Overlaid impedance measurements represented as (**a**) Bode plot; (**b**) Phase plot; and Nyquist plots for Labskin (**c**) and human skin (**d**); Measurements were obtained impedimetrically from the tattoo sensor on 8 human participants (female—orange; male—blue) and on Labskin (black).

The Bode plot (Figure 3a) reveals that Labskin had a lower impedance measurement compared to human skin. This indicates that Labskin is less resistive than human skin. This result was validated by TDC measurements (Figure 4), which showed Labskin to have a higher TDC (56.3 ± 5.7) than human skin (Male TDC: 36.0 ± 4.0 female TDC: 29.9 ± 2.1). These results were within the normal range for human skin, where men typically display a higher TDC than women (Figure 2b) [30]. Yamamoto et al. were first to investigate and elucidate the electrical properties of the SC using impedance spectroscopy, and showed that the SC layer forms a highly resistant current barrier zone in human skin [31]. The electrical properties of skin have since been widely studied and it is well established that the impedance of the skin resides within the SC, and changes in the structure or composition of the SC via chemical or mechanical impairment will alter the electrical response of skin [32,33]. The lower impedimetric signal seen for Labskin (Figure 3a) indicates that the LSE system can maintain homeostasis to a certain degree, but was not completely similar to the upper keratin layers of the human SC, which is a highly resistive barrier functioning as a more dynamic and complex system [34]. The phase plot (Figure 3b) revealed a lower phase angle for Labskin compared to human skin. It has been suggested that a higher phase angle can be indicative of healthier cell membranes in the context of wound healing in vivo, however, this requires further investigation in HSEs to understand the implications of phase angle in studies in vitro [35,36].

From the Nyquist plot (Figure 3c), the impedance spectrum of Labskin is shown, where a high frequency semi-circle is observed together with the beginning of another semi-circle at lower frequencies. The lower frequency range can be attributed to the electrode-skin interface, and the higher frequency range to the skin itself. Figure 3d shows the impedance spectrum for human skin which formed a single semi-circle with a larger diameter to that of Labskin due to the high impedance of the SC in human skin as well as potentially the impedance given by the electrode-skin interface (i.e., due to lower level of conformal contact of the tattoo with human skin) [12]. It is interesting to note that in the human skin spectra, the diameter of the semi-circle is smaller for the male skin when compared to the female skin. This correlates with the TDC measurement where a difference in TDC level was found for female vs male skin (Figure 2b). This is the subject of further research within our group. Overall, high capacitive effects were observed in human skin compared to Labskin (Figure 3c,d) and are attributed to the laminated keratin layers of the SC forming a highly resistive barrier in human skin. It is challenging to deconvolute the impedance spectra in the case of the human skin to ascertain the influence of the electrode-skin impedance from skin impedance across the spectrum. Overall however, this study highlights the potential sensitivity of tattoo electrodes, and impedance spectroscopy as a transduction technique, to investigate barrier properties in HSEs. It will become important to further investigate the electrical behaviours of both human skin and HSEs going forward. It is important to note that the manual handling involved in tattoo removal from the HSE limited the number of repeat measurements that could be performed before the model was compromised, thus necessitating further materials development to reduce mechanical impact of this type of measurement on in vitro models in the future.

Establishing an understanding of these biophysical properties and their normal range is important as it provides a baseline for future research, and has relevance for studies into areas ranging from product testing to skin physiology, the microbiome and barrier function where environmental conditions, pH, TDC and gender can play a pivotal role [37].

3.2. Volatile Organic Compounds

Characterisation of VOCs showed there to be a variety of classes of compounds emanating from human skin and Labskin. Figure 4 shows an overlay of the typical total ion chromatograms obtained, where there are distinct differences evident between human and Labskin volatile samples. There were 27 compounds identified present in participants' skin (Table 1) and 16 in Labskin (Table 2), with confirmation of compound identities performed using retention indices (RI) with a tolerance of ±10 RI

units. Compounds attributed to exogenous sources (e.g., siloxanes from SPME fibres) were excluded from these tables.

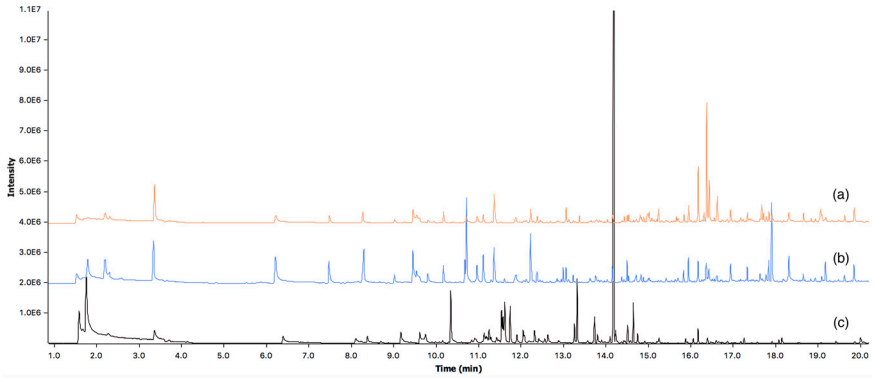

Figure 4. Overlaid total ion chromatograms showing recovered headspace solid-phase microextraction (HS-SPME) volatiles from (**a**) Female participant's skin (F1); (**b**) Male participant's skin (M1); and (**c**) Labskin.

There were 5 compounds common to the volatile profile of all human participants on at least 5 of the 6 days investigated, with 1 (decanal) and 3 (2-ethyl-1-hexanol, nonanal, geranyl acetone) compounds common on all days to all male and female participants respectively (Table 1). They include some of the most frequently reported compounds present in skin, such as geranyl acetone, 6-methyl-5-hepten-2-one, octanal, nonanal and decanal [24]. Other compounds showing a high frequency of occurrence included hexane, nonanoic acid, dodecanal and 2-ethyl-1-hexanol. 2-ethyl-1-hexanol is frequently seen in human skin VOCs, and has been linked to industrial origins [24]. Figure S1 shows the representative distribution of compound classes identified in each participant's skin volatiles. Alcohols and aldehydes remain the dominant species, accounting for 5–84% and 13–52% of the total distribution respectively. Esters also represented a significant component (up to 33%) of the female participant's VOC profile, while hydrocarbons comprised a significant component (up to 41%) of the male participant's VOCs.

Human skin is a constant source of VOCs and the dynamic nature of skin results in fluctuations in individuals' day-to-day volatile profiles. This can be due to physiological and environmental influences, which can impact the chemical composition in the skin HS. Varying levels of fatty acids and sebaceous secretions in the SC (and their rate of oxidative degradation) can account for fluctuations in the major components of endogenous VOCs. The presence of the ester methyl dihydrojasmonate (hedione) in all female participants' skin is likely due to frequent use of fragrance or cosmetics on the forearms (see Table 1). β-ionone seen in F1, F2, F3 and F4's skin has also been reported present in skin VOCs, and may be linked with cosmetics or diet [15], along with α-isomethyl ionone seen in both male and female participants' skin. It is impractical to completely eliminate such exogenous compounds from skin VOC samples due to their pervasive use in cosmetic products, which remain on skin despite using pre-treatment protocols prior to sample collection [24,38].

Table 1. Compounds identified in the skin headspace of human participants after 15 min headspace sample collection by solid-phase microextraction (SPME) followed by thermal desorption to gas chromatography-mass spectrometry (GC–MS), in order of increasing retention time. (× indicates the presence of a compound in a sample).

Compound	CAS	F1, Day:						F2, Day:						F3, Day:						F4, Day:					
		1	3	6	7	8	10	1	3	6	7	8	10	1	3	6	7	8	10	1	3	6	7	8	10
Hexane	110-54-3	×	×		×	×	×				×														
Hexanal	66-25-1																								
1-Nonene	124-11-8		×		×			×	×																
Heptanal	111-71-7	×			×											×								×	
Benzaldehyde	100-52-7	×		×	×			×	×	×	×	×	×	×	×			×	×	×	×	×	×	×	×
Octanal	124-13-0	×	×	×	×	×	×	×	×	×	×	×	×	×	×	×	×	×		×	×	×	×	×	×
2-ethyl-1-hexanol	104-76-7	×	×	×	×	×	×	×	×	×	×	×	×	×	×	×	×	×	×	×	×	×	×	×	×
Benzyl alcohol	100-51-6							×	×	×	×	×	×	×	×	×	×	×	×	×	×	×	×	×	×
1-Octanol	111-87-5		×	×		×	×	×	×	×	×	×	×	×	×	×				×		×	×	×	×
Nonanal	124-19-6	×	×	×	×	×	×	×	×	×	×	×	×	×	×	×	×	×	×	×	×	×	×	×	×
Decanal	112-31-2	×	×		×	×	×	×	×	×	×	×	×	×	×	×	×	×	×	×	×	×	×	×	×
Nonanoic acid	112-05-5		×	×	×			×	×	×	×	×	×	×	×	×	×	×	×	×	×	×	×	×	×
Undecanal	112-44-7							×	×	×	×	×	×	×	×	×	×	×	×	×	×		×	×	×
Dodecanal	112-54-9	×	×	×	×	×	×	×	×	×	×	×	×	×	×	×	×	×				×	×	×	
Geranyl acetone	689-67-8	×	×	×	×	×	×	×	×	×	×	×	×	×	×	×	×	×	×	×	×	×	×	×	×
Undecanoic acid	112-37-8								×	×	×		×	×		×						×	×	×	
α-Isomethyl ionone	127-51-5	×	×	×	×	×	×	×						×	×	×	×		×						
β-Ionone	14901-07-6	×		×				×				×	×	×	×			×	×				×		
Pentadecane	629-62-9		×			×	×							×						×	×				
Lilial	80-54-6	×	×	×	×		×			×				×			×	×				×			
Dodecanoic acid	143-07-7		×	×				×	×	×	×	×	×	×	×	×	×	×	×	×	×	×	×	×	×
Hedione	24851-98-7	×	×	×	×		×						×	×						×					
Octyl ether	629-82-3																								
Tetradecanoic acid	544-63-8		×					×	×	×	×	×	×			×	×	×	×	×	×	×	×	×	×
Octyl octanoate	2306-88-9	×	×		×	×		×	×	×	×	×	×							×					
Isopropyl palmitate	142-91-6							×	×	×	×		×	×		×	×	×		×	×	×	×		×
Oleic acid	112-80-1								×	×	×		×		×	×	×	×			×	×	×	×	×

Table 1. *Cont.*

Compound	CAS	M1, Day:						M2, Day:						M3, Day:						M4, Day:					
		1	3	6	7	8	10	1	3	6	7	8	10	1	3	6	7	8	10	1	3	6	7	8	10
Hexane	110-54-3	×	×	×	×	×	×																		
Hexanal	66-25-1							×		×	×							×							
1-Nonene	124-11-8	×	×		×	×	×	×	×	×										×	×				
Heptanal	111-71-7	×			×	×	×																		
Benzaldehyde	100-52-7	×		×	×	×	×	×		×	×	×	×	×	×	×	×		×	×	×	×	×	×	×
Octanal	124-13-0	×	×	×	×	×	×	×	×	×	×			×	×	×	×	×	×	×	×	×	×	×	×
2-ethyl-1-hexanol	104-76-7	×	×	×		×	×	×	×	×	×	×	×	×	×	×	×	×	×	×	×	×	×	×	×
Benzyl alcohol	100-51-6					×	×	×	×	×	×	×	×	×	×	×	×	×		×	×	×	×	×	×
1-Octanol	111-87-5	×	×	×	×			×		×	×			×	×					×	×	×	×		×
Nonanal	124-19-6	×	×	×	×	×	×	×	×	×	×		×	×	×	×	×	×	×	×	×	×	×	×	×
Decanal	112-31-2	×	×	×	×	×	×	×	×	×	×	×	×	×	×	×	×	×	×	×	×	×	×	×	×
Nonanoic acid	112-05-5	×	×		×	×	×	×	×	×	×		×	×	×	×	×	×	×	×	×	×	×	×	×
Undecanal	112-44-7							×	×	×	×		×	×	×	×	×	×	×	×	×	×	×		×
Dodecanal	112-54-9		×	×	×	×	×	×	×	×			×		×		×	×	×	×	×	×	×	×	×
Geranyl acetone	689-67-8	×	×	×	×	×	×	×	×	×		×	×	×	×	×	×	×	×	×	×	×	×	×	×
Undecanoic acid	112-37-8								×							×		×					×		
α-Isomethyl ionone	127-51-5	×		×		×										×	×	×	×			×	×		
β-Ionone	14901-07-6																								
Pentadecane	629-62-9	×	×		×	×		×						×											
Lilial	80-54-6		×	×		×																			
Dodecanoic acid	143-07-7	×	×	×	×	×	×	×	×	×	×		×	×	×	×	×	×	×	×	×	×	×	×	×
Hedione	24851-98-7																								
Octyl ether	629-82-3					×	×																		
Tetradecanoic acid	544-63-8		×	×	×	×	×	×	×	×	×	×	×	×	×	×	×	×	×	×	×	×	×	×	×
Octyl octanoate	2306-88-9					×															×				
Isopropyl palmitate	142-91-6							×	×	×	×			×	×	×	×		×	×	×	×	×		×
Oleic acid	112-80-1									×	×				×	×	×	×			×	×	×		

Table 2. Compounds identified in the headspace of Labskin after 15 min headspace sample collection by SPME followed by thermal desorption to GC–MS, in order of increasing retention time. (× indicates the presence of a compound in a sample).

Compound	CAS	Day					
		1	3	6	7	8	10
Ethylbenzene	100-41-4	×					
Styrene	100-42-5	×	×	×	×	×	×
Camphene	79-92-5		×				×
Decane	124-18-5	×					
Octanal	124-13-0					×	
2-Ethyl-1-hexanol	104-76-7	×	×	×	×	×	×
Undecane	1120-21-4	×					×
Nonanal	124-19-6						×
1-Nonanol	143-08-8	×	×	×	×	×	×
Camphor	76-22-2	×					
2,2,4-trimethyl-1,3-pentanediol	144-19-4		×		×	×	
Isoborneol	124-76-5						×
Dodecane	112-40-3	×	×	×	×	×	×
Isobornyl acrylate	5888-33-5	×	×	×	×	×	×
2,6-Diisopropylnaphthalene	24157-81-1	×					
n-Hexadecanoic acid	57-10-3						×

There were 5 compounds common to the Labskin VOC profile on all days investigated (Table 2). These were styrene, 2-ethyl-1-hexanol, 1-nonanol, dodecane, and isoborny acrylate. A similar variety of compound classes to that present in human skin were found present (i.e., acids, aldehydes, alcohols, hydrocarbons, esters), with the addition of terpenic compounds (e.g., camphene, camphor, isoborneol), however the individual compounds and their relative distribution varied substantially between human skin and Labskin (Figures S1 and S2). Esters comprised the largest portion of the volatile profile (80–85%) followed by acids and aldehydes (both accounting for between 3–15%) and terpenes (up to 2%). Aldehydes and acids were only detected present on Days 8 and 10, and collectively accounted for <1% of volatile profiles on those days. Aldehydes (including nonanal), alcohols and acids have previously been reported present in volatile emissions from human cells (normal melanocyte and melanoma cells) cultured in vitro [39] and were attributed to cellular metabolism. There were 3 compounds common to both human and Labskin VOC profiles herein (octanal, nonanal, 2-ethyl-1-hexanol). A number of the compounds present in Labskin VOCs (Table 2) have previously been reported present in samples from human skin, including octanal, undecane and nonanal which were listed within the 25 compounds most frequently isolated from headspace samples of human skin [24], as well as n-hexadecanoic acid [22], camphor [38] and nonanol [40]. However, it is important to note that several compounds identified (including ethylbenzene, styrene and isobornyl acrylate) likely derive from exogenous sources such as environmental contamination, the growth medium or matrix, and 2-ethyl-1-hexanol, which is a phthalate degradation product [39]. Numerous compounds identified in previous cellular VOC studies appear not to be from cellular metabolism, but are instead derived from exogenous sources such as the growth medium or environmental contaminants. Acevedo et al. similarly reported the presence of styrene and 2-ethyl-1-hexanol in human skin cell volatiles [41] where they investigated monolayer (2D) vs. 3D matrix immobilised cultures of human dermal fibroblasts and identified 6 out of total 13 separated compounds. Bartolazzi et al. investigated volatiles in human tumour cells and identified 14 compounds [42], including several exogenous compounds (e.g., butylated hydroxytoluene), which may be an additive of the growth medium [39].

Developing an understanding of typical VOC emissions in HSEs is important in establishing a baseline for future research and product testing. This technique holds significant potential for product development and testing [16]; wherein different VOC profiles and compound distributions can have implications for fragrance diffusion and perception; as well as for cosmetic dermatology in terms of

barrier function research [22]. These are both under current investigation within our research group, through evaluation of fragrance diffusion on different skin types, and a clinical study into volatiles in chronic skin disease. Sampling volatile emissions from skin in vitro and in vivo can provide valuable insights into metabolism and physiology [39,41,42], however, there is a need for detailed evaluation of environmental contaminants and matrix contributions in future development of this technique. The importance of gender differences [31,43] along with localised and temporal variations demand consideration towards permitting comparability between in vitro models and human participants.

4. Conclusions

The present research has investigated the application of two emerging tools to the repeated non-invasive assessment of skin barrier properties in vitro and in vivo. VOC profiling offers a non-contact method of biochemical interrogation that is repeatable and easily performed on both cellular models and human participants. Temporary tattoo sensors were also shown to permit non-invasive characterisation of the barrier properties in vivo and in vitro, however, the repeatability of testing in vitro did not extend beyond several hours, owing to the manual handling involved in the removal of tattoo sensors after use. The continued development of these non-invasive tools for assessment of SBF offers potential for improved quality and relevance of data, reduced ethical concerns and non-destructive sampling. There is also the potential for detection of changes that are undetectable in the traditional palpable and visual assessment, which may permit early detection of irritant reactions in cosmetic and skincare testing. This technology has significance for a variety of application areas outside that of cosmetic product testing, including clinical diagnostics, management of therapies, fundamental cell biology and physiology research.

Supplementary Materials: The following are available online at www.mdpi.com/2079-9284/4/4/44/s1, Figure S1: Distribution of compound classes in human skin volatile samples, Figure S2: Distribution of compound classes in volatile samples from human skin equivalent.

Acknowledgments: The authors would like to acknowledge Science Foundation Ireland for financial support through grant 13/CDA/2155.

Author Contributions: E.D., K.D.G. and A.M. conceived and designed the experiments; E.D. and K.D.G. performed the experiments; R.W. and R.M. performed the cell culture work; E.D. and K.D.G. analysed the data. E.D. wrote the paper.

Conflicts of Interest: The authors declare no conflict of interest. The founding sponsors had no role in the design of the study; in the collection, analyses, or interpretation of data; in the writing of the manuscript, and in the decision to publish the results.

References

1. Roberts, M.S.; Danick, Y.; Prow, T.W.; Thorling, C.A.; Grice, J.J.; Robertson, T.A.; König, K.; Becker, W. Non-invasive imaging of skin physiology and percutaneous penetration using fluorescence spectral and lifetime imaging with multiphonon and confocal microscopy. *Eur. J. Pharm. Biopharm.* **2011**, *77*, 469–488. [CrossRef] [PubMed]
2. Richters, R.J.H.; Falcone, D.; Uzunbajakave, N.E.; Varghese, B.; Caspers, P.J.; van Erp, P.E.; van de Kerkhof, P.C. Sensitive skin: Assessment of the skin barrier using confocal Raman microspectroscopy. *Skin Pharmacol. Physiol.* **2017**, *30*, 1–12. [CrossRef] [PubMed]
3. Fink, C.; Haenssle, H.A. Non-invasive tools for the diagnosis of cutaneous melanoma. *Skin Res. Technol.* **2017**, *23*, 261–271. [CrossRef] [PubMed]
4. Bandodkar, A.J.; Wang, J. Non-invasive wearable electrochemical sensors: A review. *Trends Biotechnol.* **2014**, *32*, 363–371. [CrossRef] [PubMed]
5. Lin, L.L.; Nufer, K.L.; Tomihra, S.; Prow, T.W. Non-invasive nanoparticle imaging technologies for cosmetic and skin care products. *Cosmetics* **2015**, *2*, 196–210. [CrossRef]
6. Bielfeldt, S.; Buttgereit, P.; Brandt, M.; Springmann, G.; Wilhelm, K.P. Non-invasive evaluation techniques to quantify the effects of cosmetic anti-cellulite products. *Skin Res. Technol.* **2008**, *14*, 336–346. [CrossRef] [PubMed]

7. Rogiers, V.; Balls, M.; Basketter, D.; Berardesca, E.; Edwards, C.; Elsner, P.; Ennen, J.; Lévêque, J.L.; Lóden, M.; Masson, P.; et al. The potential use of non-invasive methods in the safety assessment of cosmetic products. *ATLA* **1999**, *27*, 515–537. [PubMed]
8. Antonov, D.; Schliemann, S.; Elsner, P. Methods for the assessment of barrier function. In *Skin Barrier Function*; Agner, T., Ed.; Karger: Basel, Switzerland, 2016. [CrossRef]
9. Hammcock, M.L.; Chortos, A.; Tee, B.C.; Tok, J.B.; Bao, Z. The evolution of electronic skin (e-skin): A brief history, design considerations and recent progress. *Adv. Mater.* **2013**, *25*, 5997–6038. [CrossRef] [PubMed]
10. Jia, W.; Bandodkar, A.J.; Valdés-Ramírez, G.; Windmiller, J.R.; Yang, Z.; Ramírez, J.; Chan, G.; Wang, J. Electrochemical tattoo biosensors for real-time noninvasive lactate monitoring in human perspiration. *Anal. Chem.* **2013**, *85*, 6553–6560. [CrossRef] [PubMed]
11. Bandodkar, A.J.; Jia, W.; Yardimci, C.; Wang, X.; Ramirez, J.; Wang, J. Tattoo-based noninvasive glucose monitoring: A proof-of-concept study. *Anal. Chem.* **2014**, *87*, 394–398. [CrossRef] [PubMed]
12. De Guzman, K.; Morrin, A. Screen-printed tattoo sensor towards the non-invasive assessment of the skin barrier. *Electroanalysis* **2017**, *29*, 188–196. [CrossRef]
13. Ackmann, J.J.; Seitz, M. Methods of complex impedance measurements in biologic tissue. *Crit. Rev. Biomed. Eng.* **1984**, *11*, 281–311. [PubMed]
14. Shirasu, M.; Touhara, K. The scent of disease: Volatile organic compounds of the human body related to disease and disorder. *J. Biochem.* **2011**, *150*, 257–266. [CrossRef] [PubMed]
15. De Lacy Costello, B.; Amann, A.; Al-Kateb, H.; Flynn, C.; Filipiak, W.; Khalid, T.; Osborne, D.; Ratcliffe, N.M. A review of the volatiles from the healthy human body. *J. Breath Res.* **2014**, *8*, 014001. [CrossRef] [PubMed]
16. Caroprese, A.; Gabbanini, S.; Beltramini, C.; Lucchi, E.; Valgimigli, L. HS-SPME-GC-MS analysis of body odor to test the efficacy of foot deodorant formulations. *Skin Res. Technol.* **2009**, *15*, 503–510. [CrossRef] [PubMed]
17. Amann, A.; Smith, D. *Volatile Biomarkers: Non-Invasive Diagnosis in Physiology and Medicine*; Elsevier: Amsterdam, The Netherlands, 2013; ISBN 9780444626202.
18. Prada, P.A.; Furton, K.G. Human scent detection: A review of its developments and forensic applications. *Rev. Cien. Forenses* **2008**, *1*, 81–87.
19. Dormont, L.; Bessière, J.-M.; McKey, D.; Couhet, A. New methods for field collection of human skin volatiles and perspectives for their application in the chemical ecology of human-pathogen-vector interactions. *J. Expt. Biol.* **2013**, *216*, 2783–2788. [CrossRef] [PubMed]
20. Abaffy, T.; Möller, M.G.; Riemer, D.D.; Millikowski, C.; DeFazio, R.A. Comparative analysis of volatile metabolomics signals from melanoma and benign skin: A pilot study. *Metabolomics* **2013**, *9*, 998–1008. [CrossRef] [PubMed]
21. Dini, F.; Capuano, R.; Strand, T.; Ek, A.-C.; Lindgren, M.; Paolesse, R.; Di Natale, C.; Lundström, I. Volatile emissions from compressed tissue. *PLoS ONE* **2013**, *8*, e69271. [CrossRef] [PubMed]
22. Duffy, E.; Jacobs, M.R.; Kirby, B.; Morrin, A. Probing skin physiology through the volatile footprint: Discriminating emissions before and after acute barrier disruption. *Exp. Dermatol.* **2017**, *26*, 919–925. [CrossRef] [PubMed]
23. Pawliszyn, J. *Handbook of Solid-Phase Microextraction*; Elsevier: London, UK, 2012; ISBN 978-0-12-416017-0.
24. Dormont, L.; Bessière, J.-M.; Couhet, A. Human skin volatiles: A review. *J. Chem. Ecol.* **2013**, *39*, 569–578. [CrossRef] [PubMed]
25. Birgersson, U.; Birgersson, E.; Nicander, I.; Ollmar, S. A methodology for extracting the electrical properties of human skin. *Physiol. Meas.* **2013**, *34*, 723–736. [CrossRef] [PubMed]
26. Wenig, P.; Odermatt, J. OpenChrom: A cross-platform open source software for the mass spectrometric analysis of chromatographic data. *BMC Bioinform.* **2010**, *11*, 405. [CrossRef] [PubMed]
27. Ali, N.; Hosseini, M.; Vainio, S.; Taïeb, A.; Cario-André, M.; Rezvani, H.R. Skin equivalents: Skin from reconstructions as models to study skin development and diseases. *Br. J. Dermaotl.* **2015**, *173*, 391–403. [CrossRef] [PubMed]
28. Matousek, J.L.; Campbell, K.L. A comparative review of cutaneous pH. *Vet. Dermatol.* **2002**, *13*, 293–300. [CrossRef] [PubMed]
29. Holland, D.B.; Bojar, R.A.; Jeremy, A.H.T.; Ingham, E.; Holland, K.T. Microbial colonization of an in vitro model of a tissue engineered human skin equivalent—A novel approach. *FEMS Microbiol. Lett.* **2008**, *279*, 110–115. [CrossRef] [PubMed]

30. Mayrovitz, H.N.; Carson, S.; Luis, M. Male-female differences in forearm skin tissue dielectric constant. *Clin. Physiol. Funct. Imaging* **2010**, *30*, 328–332. [CrossRef] [PubMed]
31. Yamamoto, T.; Yamamoto, Y. Electrical properties of the epidermal stratum corneum. *Med. Biol. Eng.* **1976**, *14*, 151–158. [CrossRef] [PubMed]
32. White, E.A.; Orazem, M.E.; Bunge, A.L. Characterization of damaged skin by impedance spectroscopy: Mechanical damage. *Pharm. Res.* **2013**, *30*, 2036–2049. [CrossRef] [PubMed]
33. White, E.A.; Orazem, M.E.; Bunge, A.L. Characterization of damaged skin by impedance spectroscopy: Chemical damage by dimethyl sulfoxide. *Pharm. Res.* **2013**, *30*, 2607–2624. [CrossRef] [PubMed]
34. Baroni, A.; Buommino, E.; De Gregoria, V.; Ruocco, E.; Ruocco, V.; Wolf, R. Structure and function of the epidermis related to barrier properties. *Clin. Dermatol.* **2012**, *30*, 257–262. [CrossRef] [PubMed]
35. Lukaski, H.C.; Moore, M. Bioelectrical impedance assessment of wound healing. *J. Diabetes Sci. Technol.* **2012**, *6*, 209–212. [CrossRef] [PubMed]
36. Swisher, S.L.; Lin, M.C.; Liao, A.; Leeflang, E.J.; Khan, Y.; Pavinatto, F.J.; Mann, K.; Naujokas, A.; Young, D.; Roy, S.; et al. Impedance sensing device enables early detection of pressure ulcers in vivo. *Nat. Commun.* **2015**, *6*, 6575. [CrossRef] [PubMed]
37. Kim, M.K.; Patel, R.A.; Shinn, A.H.; Choi, S.Y.; Byun, H.J.; Park, K.C.; Youn, S.W. Evaluation of gender difference in skin type and pH. *J. Detmatol. Sci.* **2006**, *41*, 153–156. [CrossRef] [PubMed]
38. Gallagher, M.; Oysocki, C.J.; Leyden, J.J.; Spielman, A.I.; Sun, X.; Preti, G. Analyses of volatile organic compounds from human skin. *Br. J. Dermatol.* **2008**, *159*, 780–791. [CrossRef] [PubMed]
39. Kwak, J.; Gallagher, M.; Ozdener, M.H.; Wysocki, C.J.; Goldsmith, B.R.; Isamah, A.; Faranda, A.; Fakharzadeh, S.S.; Herlyn, A.T.; Johnson, C.; et al. Volatile biomarkers from human melanoma cells. *J. Chromatogr. B* **2013**, *931*, 90–96. [CrossRef] [PubMed]
40. Curran, A.M.; Ramirez, C.F.; Schoon, A.A.; Furton, K.G. The frequency of occurrence and discriminatory power of compounds found in human scent across a population determined by SPME-GC/MS. *J. Chromatogr. B* **2007**, *846*, 86–97. [CrossRef] [PubMed]
41. Acevedo, C.A.; Sánchez, E.Y.; Reyes, J.G.; Young, M.E. Volatile organic compounds produced by human skin cells. *Biol. Res.* **2007**, *40*, 347–355. [CrossRef] [PubMed]
42. Bartolazzi, A.; Santonico, M.; Pennazza, G.; Martinellli, E.; Paolesse, R.; D'Amico, A.; Di Natale, C. A sensor array and GC study about VOCs and cancer cells. *Sens. Actuators B* **2010**, *146*, 483–488. [CrossRef]
43. Penn, D.J.; Oberzaucher, E.; Grammer, K.; Fischer, G.; Soini, H.A.; Wiesler, D.; Novotny, M.V.; Dixon, S.J.; Xu, Y.; Brereton, R.G. Invididual and gender fingerprints in human body odour. *J. R. Soc. Interface* **2007**, *4*, 331–340. [CrossRef] [PubMed]